Nanographite · nanocomposites · reinforcing properties · Huber-Vilgis plot

It was studied the effect of surface area (s.a.) of nanosized graphites on dynamic-mechanical and tensile properties of nanocomposites based on poly (styrene-*co*-butadiene) as the polymer matrix. Nanographite with very high s.a. (>800 m²/g) was compared with graphites with low s.a. (<40 m²/g). All nanographites had remarkable in plane crystallinity and the high s.a. graphite was characterized by a lower number of layers stacked in crystalline domain. Results of this work demonstrate that nanosized graphite leads to re-markable improvement of the mechanical reinforcement of elastomeric composites and suggest, to some extent surprisingly, that moderate s.a. should be selected, particularly to have moderate dissipation of energy.

Einfluss der Nano-Graphit Oberfläche auf die mechanische Verstärkung von Nano-Kompositen basierend auf Poly (styrol-co-butadien)

Nano-Graphit · Nano-Komposite · Verstärkungseigenschaften · Huber-Vilgis plot

Es wurde der Effekt der spezifischen Oberfläche von nanoskaligen Graphit auf die dynamisch-mechanischen Eigenschaften und auf die Dehneigenschaften von auf Poly(styrol-*co*-Butadien) basierenden Nano-Kompositen als Polymermatrix untersucht. Nano-Graphit mit einer sehr hohen Oberfläche (>800 m²/g) wurde mit Graphiten mit niedriger Oberfläche (>40 m²/g) verglichen. Alle Nano-Graphite hatten eine bemerkenswerte Kristallinität, wobei der Graphit mit hoher Oberfläche durch eine niedrigere Anzahl von geschichteten Lagen in den kristallinen Einheiten gekennzeichnet war. Die Ergebnisse zeigen, dass nanoskaliger Graphit zu einer höheren Verstärkung und zu einer moderaten Energiedissipation beiträgt.

Figures and Tables:
By a kind approval of the authors.

Influence of Nanographite Surface Area on mechanical Reinforcement of Nanocomposites based on Poly(styrene-co-butadiene)

1. Introduction

"Nanofillers" are fillers whose particles have at least one dimension below 100 nanometers and that can be individually dispersed into a polymer matrix [1]. On the basis of their geometry, they can have all three dimensions (e.g. fumed silicon dioxide) or two dimensions (e.g. graphene) or one dimension (e.g. clay minerals, mica) in nanometer range.

Over the last years, nanofillers have been employed to promote the reinforcement of polymer matrices. Reports are available in the scientific literature on nanocomposites based on nanofillers such as clay minerals [2-8] carbon nanotubes [9-10], graphene and graphitic nanofillers made by few layers of graphene [11-13]. Such nanofillers are characterized by high aspect ratio and high surface area (s.a.), thus allowing a high interfacial area and remarkable interaction with the polymer matrix, with profound effect on the dynamic-mechanical and tensile properties of nanocomposites. Remarkable increase of the initial modulus of elastomers has been reported, for clays [2-8, 14-17], carbon nanotubes [9-10. 18-19], and graphitic nanofillers [20-22]. However, it is widely acknowledged that such effect diminishes and fails as the strain amplitude increases [14-22]. Nanofillers have indeed high s.a. but do not have the so called structure[23] that means they are not able to occlude rubber chains; hence they are not able to transform them into a rigid undeformable phase. In the light of these findings, nanofillers with high s.a. promote a remarkable improvement of the initial modulus of elastomeric nanocomposite and, at the same time, a pronounced non linearity of the viscoelastic modulus. This is critical in view of large scale application of rubber nanocomposites, such as the one in tire compounds, as it leads to large energy dissipation[23]

It appears thus of interest to investigate nanosized fillers with high aspect ratio and, at the same time, low s.a., in order to have appreciable mechanical reinforcement and minor dissipation of energy. In this work, nanosized graphites endowed with low s.a. were studied and compared with a nanosized graphite with a very high s.a.. Preliminary data on the high s.a. graphite have been already presented [21-22]. Surface properties of each nano-graphite were investigated through sorption measurements. Morphology was studied by means of scanning electron microscopy (SEM) and crystalline structure through wide angle X-ray diffraction (WAXD). Composites were prepared with poly(styrene-co-butadiene) as the rubber matrix, with the nanographite in a wide range of content. Dy-

Authors

V. Kumar, R. Scotti, T. Hanel, L. Giannini, M. Galimberti
Milano, Italy, U. Giese,
Hannover, Germany

Corresponding authors:
V. Kuma
Dipartimento di Scienza dei Materialie Pirelli-CORIMAV, Università degli Studi di Mi-lano-Bicocca, Viale R. Cozzi 53, 20126, Milano, Italy.
E-Mail: v.kumar@campus.unimib.it

U. Giese
Elastomer Chemistry, Deutsches Institut für Kautschuktechnologie e.V. (DIK e.V.) Eupener Straße 33, D-30519, Hannover, Germany.
E-Mail: ulrich.giese@dikautschuk.de

M. Galimberti
Dipartimento CMIC "G. Natta", Politecnico di Milano,
Via Mancinelli-7, Milano, Italy.
E-Mail: maurizio.galimberti@polimi.it

1 Formulations of nanocomposites with graphitic nanofillera

Poly(styrene-co-butadiene) rubber: 100							
Nano-graphite	2	4	8	12	16	20	30	40
Other ingredients: ZnO – 4, stearic acid – 2, sulphur – 2, CBS – 1							

[a]amount of ingredients is expressed in phr

namic-mechanical as well as tensile properties were investigated. This work is a part of the research aimed at answering the following question: is it useful to have high surface area, for graphite as filler of a rubber compound, to improve the properties of such compound? Attention of this work was on the mechanical reinforcement.

2. Experimental

2.1. Materials

Poly(styrene-co-butadiene) rubber (SBR) from anionic solution polymerization had trade name Buna VSL 2525-0 M (25% styrene and 25% vinyl), Mooney viscosity (ML_{1+4}) of 54 and T_g of -49°C and was purchased from Lanxess Deutschland AG. Commercially available graphitic nanofillers were: SFG6 and KS4 from TIMCAL, EXG 9840 from Kropfmühl AG Deutschland and xg C750 from XG science. Other ingredients used were: zinc oxide, stearic acid, cyclohexyl benzothiazol-2-sulfenamide (CBS) and sulphur from Sigma-Aldrich. All materials were used as received without any further treatment.

2.2. Graphitic Nanofiller Characterization

Adsorption isotherm measurements:
They were performed using BELSORP-max (BEL, Japan Inc.) volumetric adsorption instrument. Published experimental procedure was adopted [24]. Moisture was removed before measurements by pre-heating the samples at 300 °C. Nitrogen gas was infused for measuring BET surface area.

Scanning electron microscope (SEM):
Measurements were performed using Zeiss EVO MA 10, equipped with tungsten filament and carried out at a controlled voltage of 8 kV.

Wide-angle X-ray diffraction (WAXD):
XRD-patterns were obtained through an automatic Bruker D8 advanced diffractometer operated at 35 kV and 40 mA using Ni filtered Cu-K_α radiation (1.5418 Å). $D_{hk\ell}$ correlation lengths were calculated by using the Scherrer equation (Eq. 1)

$$D_{hk\ell} = K\lambda / (\beta_{hk\ell} \cos \theta_{hk\ell}) \quad (1)$$

where K is Scherrer constant, λ is wavelength of irradiating beam (1.5419 Å, CuK_α), $\beta_{hk\ell}$ is the width at half height, and $\theta_{hk\ell}$ is the diffraction angle.

The introduction of a correction factor has to be used in case $\theta_{hk\ell}$ is lower than 1°. Dimension of graphite crystallites in orthogonal and parallel directions with respect to structural layers can be estimated by calculating out-of-plane ($D\parallel$) from $D_{00\ell}$ and the in-plane ($D\perp$) from D_{hk0} patterns. In particular, D00ℓ was calculated by using the 002 reflection and Dhk0 from 110 reflections. The shape anisotropy is defined as the ratio ($D\parallel/D\perp$) between in-plane and out-of-plane correlation lengths [25].

2.3. Preparations of nanocomposites

SBR nanocomposites were prepared in a laboratory scale rheomix Haake™ 600. Formulations of nanocomposites are shown in Table 1. Amount of ingredients is expressed in parts per hundred rubber (phr).

49.5 g of SBR were introduced into the mixing chamber at 50 °C and masticated for 1-2 minutes at 60 rpm. The amount of graphitic nanofillers were then added and mixed for 4-5 minutes until a stable torque was achieved. ZnO and stearic acid were thereafter mixed for 2-3 minutes. Finally, sulphur and CBS were added and mixed for 2-3 minutes until torque reaches equilibrium before discharging nanocomposites from mixing chamber. Nanocomposites were finally homogenized by passing them on two roll open mill for 4/5 times at room temperature at nip of 1 cm between rolls.

2.4. Nanocomposites Characterizations

Study of crosslinking reaction:
Nanocomposites were cured in a Monsanto oscillating disc rheometer (MDR 2000) (Alpha Technologies, Swindon, UK), determining minimum modulus M_L, maximum modulus M_H, the time required to achieve the optimum of vulcanization, reported as t_{90}, corresponding to 90 % of the maximum torque.

Dynamic-mechanical measurements:
They were made in torsion mode by using Rubber Process Analyzer (RPA 2000, Alpha Technology). Strain sweep measurements were carried out on uncrosslinked nanocomposites at 80 °C. Samples were then kept in instrument at minimum strain amplitude (0.28 %) and frequency of 1 Hz for 300 s to achieve fully equilibrated conditions. Values of storage modulus (G' in kPa) were recorded after achieving the fully equilibrated conditions.

Stress-Strain tests:
They were performed for tensile properties according to DIN 53 504 standards on cured samples with a preload of 0.5 N using universal testing machine-Zwick / Roll Z010. Strain rate was fixed at 10 mm/minute for all investigations.

M_L, maximum value of torque, indicated as maximum modulus M_H.

3. Results and discussion

3.1. Characterization of graphitic nanofillers

Features of nano-graphites used in the present work are shown in Table 2.

Surface area was determined through BET measurements, as indicated in the experimental part and as already reported [24]. In the case of low s.a. graphite, values are in the range from about 14 to about 30 m²/g, pretty low for a nanosized carbon allotrope. In fact, nanoG such as xg C750 has s.a. as high as about 820 m2/g [21. Moreover, a value of about 300 m2/g was reported for nanosized graphite obtained through milling [20, 25].

Table 2 reports as well the out of plane correlation length ($D\perp$) and the in plane correlation length ($D\parallel$), determined from the X-ray patterns, the shape

2 Nanofiller's characteristics

S.No.	Nanofillers	Surface Area (m²/g)	D⊥ (nm)	D∥ (nm)	Shape Anisotropy	No. of Stacked Layers
1.	xg C750	817.3	9	26	2.7	24
2.	EXG 9840	39.5	~16.1	~15.9	1.0	~48
3.	KS4	23.8	16	25.6	1.6	~48
4.	SFG6	13.8	15	25.5	1.7	~45

anisotropy and the number of stacked layers, calculated from the ($D\perp$) values. These characteristics are discussed below in 3.1.2 paragraph.

3.1.1. SEM investigations

Morphology of nanoG samples was investigated by means of SEM analysis on a significative number of samples. Representative micrographs are shown in figure 1. In figure 1a and figure 1b, EXG 9840 shows "worm-like" or "accordion-like" morphology and presents graphitic layers that have film-shaped appearance with small transparent corrugations. Micrographs of KS4 are reported in figure 1c and figure 1d and micrographs of SFG6 are in figure 1e and figure 1f. Both nanoGs show "platelet-like" morphology with well defined ridge-patterns, without being exfoliated to single or very few graphene layers. Moreover, SEM micrographs show sharp edges and craters like features nearer to aggregated particles.

The higher degree of exfoliation and the corrugated nature of EXG 9840 could be due to their preparation under vigorous thermo-acidic treatments [26-27] and are in line with the higher value of s.a. Average diameters of particles consisting of stacked graphene layers are in submicron region and appear randomly oriented. Figure 1g and figure 1h show micrograph of xg C750 at lower and higher magnification respectively. The high resolution picture shows a damaged (ruptured) platelet morphology which could be due to several vigorous treatments (acidic or thermal) during preparation to achieve high s.a.. It can be also noticed the discontinuous arrangement of graphene sheets. Lateral dimension of aggregates and agglomerates is in the range from few nanometers to a submicrometric level.

3.1.2. Wide-angle X-ray diffraction (WAXD) analysis

The crystalline order of nanofillers was investigated through wide-angle X-ray diffraction (WAXD). Figure 2 presents WAXD patterns of graphitic nanofillers SFG6, KS4, EXG 9840 and xg C750. WAXD shows (00ℓ) reflections that indicate the order in the direction orthogonal to structural layers: 002 at 26.57° that corresponds to an inter-layer 0.335 nm and 004 at 54.3°. Moreover, one can detect 100 and 110 reflections, at 42.5° and 77.6° respectively, that allow to investigate the in plane order. [20,21] Among

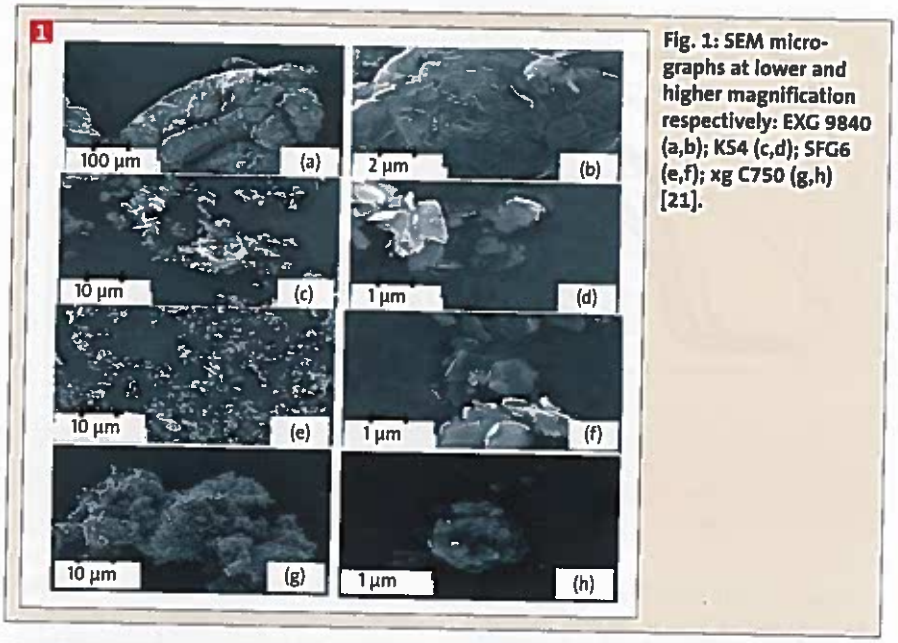

Fig. 1: SEM micrographs at lower and higher magnification respectively: EXG 9840 (a,b); KS4 (c,d); SFG6 (e,f); xg C750 (g,h) [21].

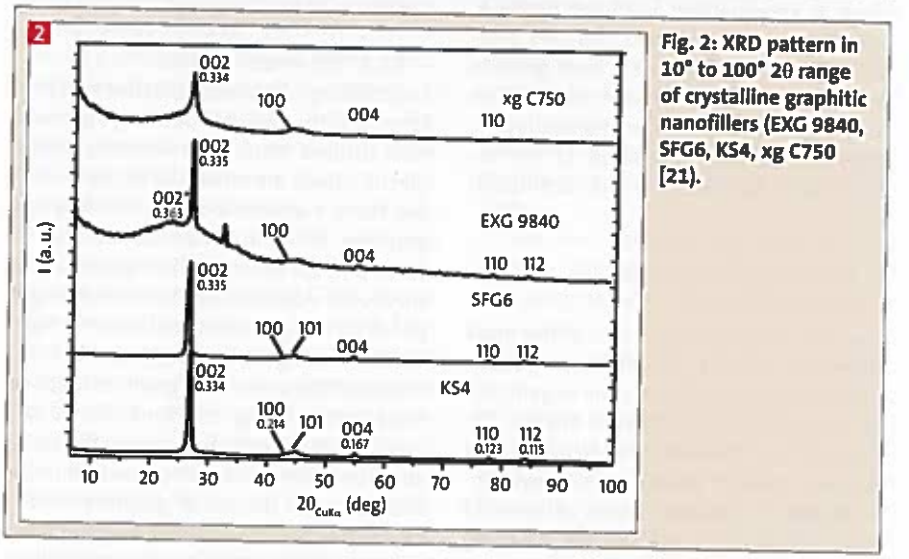

Fig. 2: XRD pattern in 10° to 100° 2θ range of crystalline graphitic nanofillers (EXG 9840, SFG6, KS4, xg C750 [21].

all the samples, only EXG 9840 reveals an appreciable amount of amorphous carbon. The out of plane correlation length ($D\perp$) and the in plane correlation length ($D\parallel$) were calculated by using (002) and (110) reflections, respectively. Data are shown in Table 2. ($D\perp$) value of xg C750 (9 nm) is very close to that (about 10 nm) reported in the literature for a nanosized graphite with 300 m²/g as s.a. [25]. Values for the low s.a. graphites appear those typical of expanded graphites, reported to be in the range from 17 nm to 20 nm [25]. D|| values of xg C750 and low s.a. graphites KS4 and SFG6 are very close to each other (about 25 nm) and only the value of EXG 9840 is lower (about 16). Largest values reported in the literature are from 30 nm to 45 nm, whereas the one typical of a carbon black (N326) is about 3 nm [25]. It appears thus that also low s.a. graphites have appreciable in plane crystalline order.

From the ($D\perp$) value and taking into consideration the interlayer distance, the number of stacked layers was calculated. Lower number was found for the graphite sample with very high s.a. However, also graphite samples with low s.a. have a relatively low number of stacked layers. The $D\perp/D\parallel$ ratio gave the shape anisotropy. The value calculated for xgC750 (2.7) is in line with the largest shape anisotropy values reported in the literature[25], that are in the range from 2.2 to 3.1 and, in particular, is not far from the highest value. Graphite samples with low s.a. are not characterized by a high shape anisotropy and this is due, as commented above, to the relatively low degree of exfoliation, rather than to a poor in plane crystalline order.

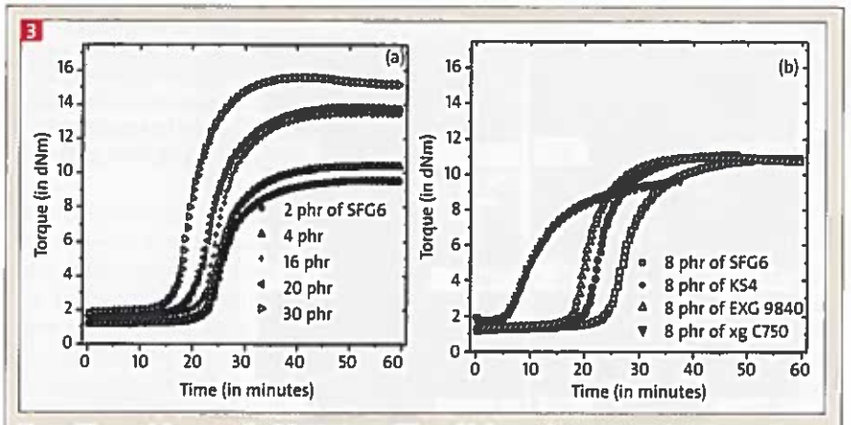

Fig. 3: Rheometric curves for (a) SFG6 nanofiller with increasing concentration from 2 to 40 phr and (b) 8 phr of SFG6, KS4, EXG 9840 and adopted data of xg C750 22 for SBR based nanocomposites.

From the structural characterization of the graphite grades selected for this work, it appears that both the high s.a. sample and at least two samples with low s.a. are made by layers with good in plane crystallinity. Moreover, all of them have a limited number of stacked layers. They can be thus compared as reinforcing fillers for elastomer nanocomposites.

3.2. Characterizations of nanocomposites

Graphite is layered filler. One of the most relevant aspects of nanocomposites based on layered fillers is the organization of such fillers in polymer matrix, dispersion and potential intercalation of polymer chains. These aspects were investigated in previous works by some of the authors. [20, 21] In particular, by means of transmission electron microscopy and XRD analyses it was observed that nano-G achieved even dispersion in the polymer matrix and that polymer chains were not intercalated in the interlayer space of nano-G, whose XRD patterns revealed (002) reflection exactly at the same 2θ value.

3.2.1. Rheometric curves

Crosslinking of nanocomposites was performed with a sulphur based system and was studied through rheometry. Rheometric curves are shown in figure 3. Curves for a nanocomposite with low s.a. graphite, SFG6, in concentration from 2 to 40 phr, are presented in figure 3a and curves for nanocomposites containing 8 phr of all the graphites are shown in figure 3b. From figure 3a, it appears that increase of the amount of graphite leads to faster crosslinking reactions and to largest values of torque. Curves in figure 3b show that the crosslinking reaction becomes faster as the s.a. of graphite increases. The occurring of faster vulcanization reaction in the presence of carbon fillers is widely acknowledged. Possible explanation is the enhancement of the thermal conductivity of the composites.

In fact, the presence of carbon filler endowed with high thermal conductivity favours the heat transfer in the composites and, in turns, reactions that occur at high temperature, such as vulcanization. The addition of vapor grown carbon fibers was claimed to reduce the vulcanization time by 8% [28]. The basic pH of the carbon filler is also considered. In this respect, it has to be mentioned that the presence of amino group on the surface of xg C750 has been reported.[21, 22] Instead, the highest value of torque appears quite similar for the low s.a. graphites and even lower for the xgC750. Phenomena such as the enhanced torque in early stage of vulcanization were not evidenced, suggesting filler flocculation does not occur.

The effect on the crosslinking reaction of graphites with low s.a. was further investigated by plotting the values of time required to achieve the optimum of vulcanization t'90 and the difference MH - ML as a function of the amount of graphite in the nanocomposite. Graphs are reported in figure 4a and in figure 4b, respectively.

Figure 4a shows that t'90 decreases almost linearly with the amount of nanographite, thus confirming what observed in figure 3a. In particular, fastest vulcanization reaction is revealed by EXG 9840 that has the largest s.a. (among the low s.a. graphites). As commented above, basic pH of the carbon filler is expected to be in favor of faster vulcanization. EXG 9840 has acidic functional groups. It could be thus commented that the effect of s.a. overcome that of the surface acidity. However, it has been reported an enhanced curing reaction for acid-graphite platelets [26,27]. Acidic groups on EXG 9840 could lead to higher energy surface heterogeneity of the filler that could favor faster crosslinking reaction. The effect of carbon allotropes on sulphur based crosslinking of elastomers deserves to be further investigated. However, faster crosslinking reaction is not necessarily appreciated in the rubber field, as it could give rise to premature scorching, worsening the processability. The addition of larger amounts of SFG6, KS4 and EXG 9840 in the rubber matrix causes the increase of torque (MH-ML,) as shown in figure 4b.

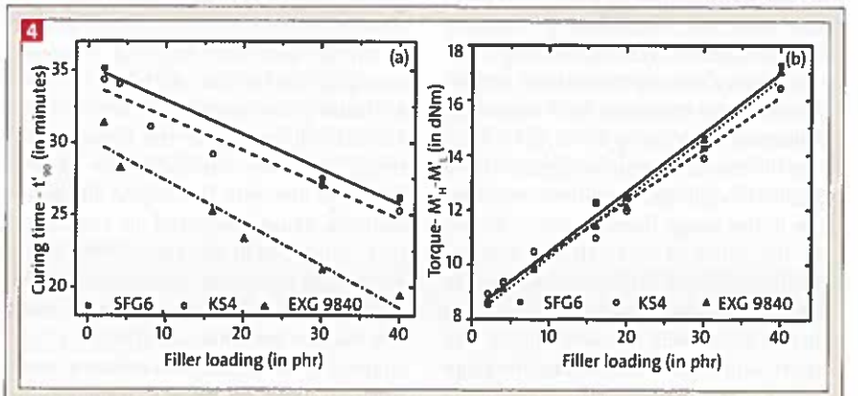

Fig. 4: (a) optimum curing time (t'_{90}) vs filler loading; (b) Torque difference ($M_H - M_L$) versus filler loading.

3.2.2. Dynamic-mechanical properties

The dependence of storage modulus G' on the strain amplitude, for graphite based nanocomposites, is shown in Figure 5.

Curves in figure 5a refer to nanocomposites with increasing amount of SGF6.

Experimental data reveal that the initial modulus of the nanocomposite strongly increases with the increase of nanographite content. This was expected on the basis of the theory of reinforcement[2-29]. Moreover, as mentioned above, nanofillers lead to remarkable enhancement of the material initial modulus and this occurs also for nanographites [19-22]. The effect of graphite particles morphology and of their preferred in-plane orientation has been hypothesized [12]. To justify the extent of modulus enhancement aspects such as nano-G dispersion and the structure of the crosslink network (density and bridges' length distribution) should be investigated.

With the increase of nanographite content, also the non linearity of the modulus, that means the Payne effect [30], is strongly enhanced. Figure 5b shows the dependence of G' on the strain amplitude for composites containing 20 phr of all the nanographites. Among the nanographites with low s.a., the one with the largest value (EXG 9840) promotes the largest Payne effect. xg C750 gives rise to the strongest G' reduction with the strain amplitude. Interpretations of Payne effect move from the filler networking concept and make reference to two main models. The first one is based on agglomeration–deagglomeration process of the filler network, above the filler percolation threshold [30-34]. The second model focuses the attention on filler–matrix interaction, hypothesizing matrix-filler bonding and debonding mechanisms [39-44]. This work has not the scope of discussing the physical mechanisms occurring in the composites. However, whatever is the origin of the Payne effect, the filler surface plays an important role [29,45].

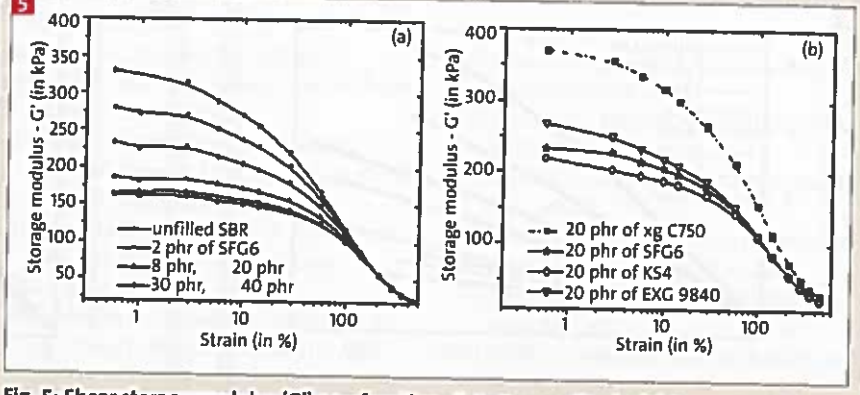

Fig. 5: Shear storage modulus (G') as a function of strains amplitude: (a) for composites with increasing concentration (from 2 to 40 phr) of SFG6; (b) for composites with 20 phr of xg C750 [22].

Nanographite xgC750 is thus expected to promote the largest Payne effect, that means the largest dissipation of energy in the composite material. Storage modulus G' at minimum strain (0.56%) is plotted as a function of nanographite content in figure 6. It can be noticed that storage modulus increases with increasing filler loading. In the case of composites based on xg C750, the increment of the modulus with the filler content appears clearly not linear and suggests two different regimes, at low and at high nanographite content, respectively. Such shift from one regime to the other can be hardly appreciated for the composites based on low s.a. graphites. The enhancement of the modulus as a consequence of filler addition can be expressed for spherical filler particles through the Smallwood-Guth-Gold equation (Equation 2) [45]:

$$G_c/G_m = 1 + 2.5\,\Phi + 14.1\Phi^2 \qquad (2)$$

where G_c is the elastic modulus of the composite, G_m is the elastic modulus of the neat elastomer, Φ is the filler volume fraction and the quadratic term accounts for the mutual disturbance of filler particles.

For non spherical particles and for particle aggregates, Guth proposed the following equation [46,47] (Equation 3):

$$G_c/G_m = 1 + 0.67f\Phi + 1.62f^2\Phi^2 \qquad (3)$$

where f is a shape factor that takes into account the rod-like shape of filler or filler aggregate and is given by the length to width ratio of particle or aggregate. Some of the authors relied on this model in previous studies on elastomer nanocomposites [14, 17, 18, 21,22], to fit the

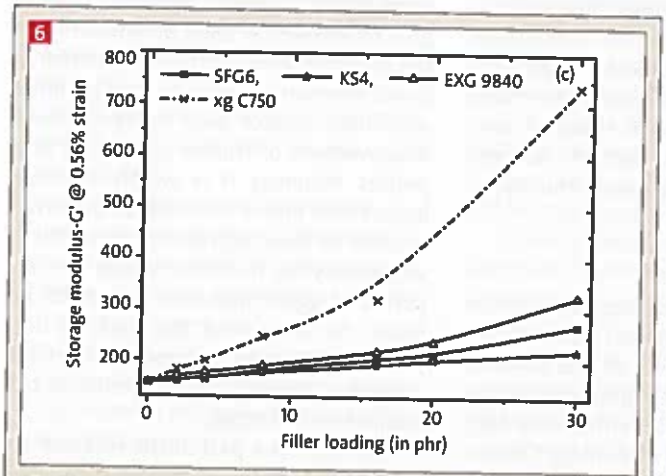

Fig. 6: Storage modulus at minimum strain (0.56%) as a function of filler loading for nanocomposites based on SFG6, KS4, EXG 9840 and 20 phr of xg C750 [22].

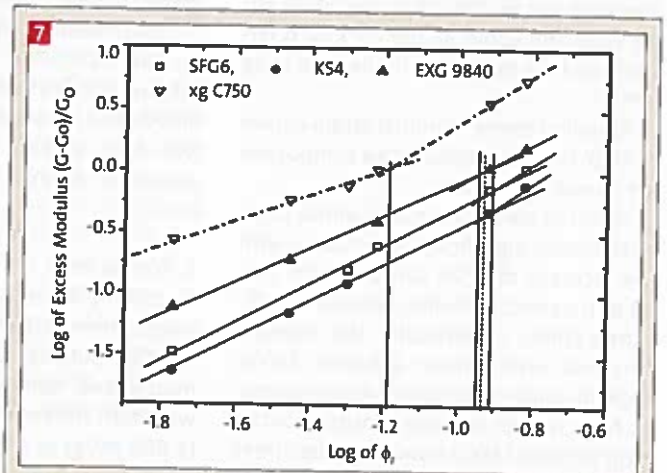

Fig. 7: Double logarithmic plot of the excess modulus, with respect to neat matrix, as a function of the nanographite volume fraction / (Huber–Vilgis plot).

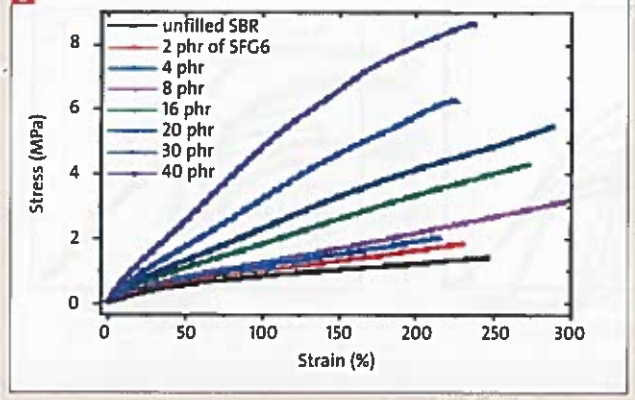

Fig. 8: Nominal stress–nominal strain curves obtained in tensile tests performed at room temperature and at a cross-head rate of 10 mm/min for SFG6 based nanocomposites.

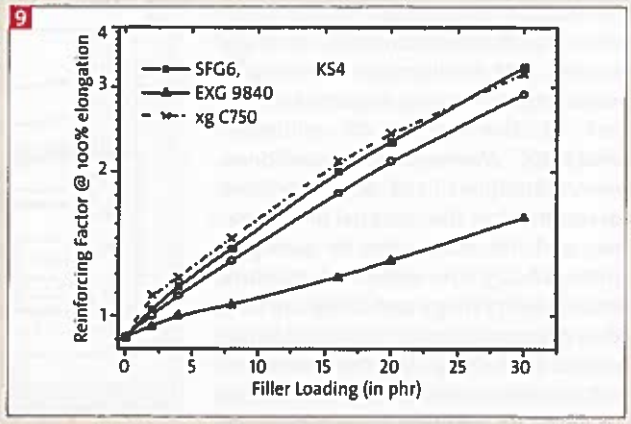

Fig. 9: Reinforcing factor ($F=\sigma_F/\sigma_0$) from stress-strain curves obtained from graphitic nanofillers (SFG6, KS4, EXG 9840) and xg C750[22] in SBR, at 100% elongation, from stress-strain measurements.

mechanical properties of nanocomposites based on PI and containing different types of nanographites.

In filled polymer melt and elastomers, the occurring of filler percolation threshold can be obtained through Huber-Vilgis double logarithmic plot by representing excess modulus ($(G\gamma_{min}-G_0)/G_0$) at lower strain amplitude as a function of filler volume fraction. Points derived from nanocomposites of this work are plotted in figure 7. Two linear regimes can be identified in the case of xg C750: the two straight lines with different slopes define the percolation threshold that was estimate to occur at 16.6 phr of nanographite. In the case of graphites with low s.a., the straight line with the higher slope can be only hypothesized. However, assuming the validity of such hypothesis, the amount of nanographite calculated for the occurring of hypothetical percolation threshold, about 28 phr for EXG 9840, about 30 phr for SFG6 and about 31 phr for KS4, is larger than that calculated in the case of xg C750.

Nominal stress–nominal strain curves of SFG6 filled SBR crosslinked composites are shown in figure 8.

It can be clearly seen that initial slope of the curve significantly increases with the increase of SFG6 content from 0 to 40 phr: nanocomposites become significantly stiffer. In particular, the increase of stress, when strain achieves 300%, appears quite remarkable. As an example, for a rubber nanocomposites containing 16 phr of SFG6 nanofiller, the stress increases from ~1.3 MPa (at 50% elongation) to ~3.5 MPa (at 200% elongation). Such enhancement indicates the even distribution and dispersion of the nanographite. Interestingly, values of stresses determined for different nanographites are quite similar to each other and are similar upto 20 phr loading to those measured for xg C750 nanocomposites [21, 22]. To assess the ability of nanographite to promote the stiffness of the composite, the reinforcing factor F, defined as the ratio between the stress of the composite and the stress of the matrix at 100% strain ($F=\sigma_F/\sigma_0$) 100%, was calculated for all the nanocomposites for every nanographite content.

The dependence of the reinforcing factor as a function of the filler loading is shown in figure 9. It can be clearly observed that the stress enhancement is quite similar for the nanocomposite based on the large s.a. graphite and on at least two low surfaces are graphites SFG6 and KS4. It appears thus that the s.a. has a minor effect on the tensile properties of graphite based nanocomposites.

Lower reinforcing factor is observed for EXG 9840. This could be hypothetically ascribed to worse dispersion of such filler in the rubber matrix. However, analysis such as SEM of fracture surfaces would be required to assess this hypothesis.

4. Conclusions

Nanocomposites were prepared with on poly(styrene-*co*-butadiene) from anionic solution polymerization as the polymer matrix and nanosized graphites endowed with different s.a., either very high (> 800 m²/g) or low (< 40 m²/g). Characterization revealed appreciable in plane crystallinity in all the nanographites, close to the highest values reported in the literature, and a lower number of layers stacked in the crystalline domain for the high s.a. graphite.

Kinetics of sulphur based crosslinking reaction was affected by nanographites: larger amount and higher s.a. led to faster reaction. Clear effect of s.a. was not observed on the highest modulus in the rheometric curve. Nanographite does have effect on the mechanical reinforcement. Storage modulus measured through dynamic-mechanical tests in the torsion mode remarkably increases with nanographite content. High s.a. leads to pronounced increase of the Payne effect. Tensile properties appeared to be similar for all the nanocomposites, in spite of the difference of s.a.

Results reported in this work throw light on the role of s.a. of a nanofiller such as a nanographite. Even in the absence of other important pieces of information, such as those arising from a morphological investigation of the nanocomposites, it seems to be possible to give an answer, at least preliminarily, to the question asked in the introduction. It is not necessarily useful to have graphite with high surface area to have overall improvement of rubber compound properties. Whereas it is widely acknowledged that high s.a. should be preferred in order to have high electrical conductivity of polymer matrices, results here reported suggest that low s.a. could be better for improving the balance between tensile and dynamic-mechanical properties, in particular for reducing the dissipation of energy.

This work is a part of the research aimed at answering the following question: is it useful to have high surface area, for graphite as nanofiller in a rubber compound, to improve the properties of

such compound? Attention of this work was on the mechanical reinforcement. To strengthen these conclusion, morphological characterization of nanocomposites. At present state of the research, these results are not available. However, data reported in the paper allow to provide a reliable answer to the question that was the main objective of the paper: is it useful to have high surface area for a graphite as a filler in a rubber compound? Are the properties of the compound improved when graphite has high surface area? What appears form the collected results is that high surface area graphite definitely leads to remarkable improvement of the Payne effect whereas improvement of mechanical reinforcement can not be detected from tensile measurements. Morphological data on the dispersion of nanofillers are at present not available and the research was performed without adopting any particular intervention in order to favour a good dispersion. However, difficult dispersion should be expected exactly for the high surface area graphite and improvement of dispersion for this type of graphite should definitely lead to the enhancement of the filler networking phenomenon that means to even larger Payne effect. On the basis of these considerations, we believe that the warning that arises from this work maintains its validity: take care of high surface area nanofillers.

Acknowledgement

Authors acknowledge "Pirelli-CORIMAV" for financial support of the work.

References

[1] British Standards Institute. Vocabulary. Nanoparticles, PAS 71:2005 [withdrawn].
[2] Alexandre M.; Dubois P, Mater. Sci. Eng., 2000, 28,1.
[3] Chen B, Evans JRG, Greenwell HC, Boulet P and Coveney PV et al Chem. Soc. Rev., 2008, **37**, 568.
[4] Paul DR and Robeson LM, Polym. Nanotechn.: Nanocompos. Polym., 2008, **49**,3187.
[5] Galimberti M., Rubber Clay Nanocomposites: Science, Technology, Applications. 1st edition, John Wiley and Sons, 2011.
[6] Galimberti M., Rubber Clay Nanocomposites, Chapter 4 in Advanced Elastomers - Technology, Properties and Applications, edited by Anna Boczkowska.
[7] Mittal V., Advances in polyolefin nanocomposites. CRC Press, Boca Raton, 2011.
[8] Maiti M., Bhattacharya M., Bhowmick A.K., Rubber Chem. Technol., **81**, 384 (2008).
[9] Moniruzzaman M., Winey KL., Macromolecules, 2006, **39**, 5194.
[10] Bokobza L., Polymer, 2007, **48**, 4907.
[11] Potts JR, Dreyer DR, Bielawski CW and Ruoff RS, Polymer, 52(5) 2011.
[12] Kumar V., Hanel T., Fleck F., Möwes M., Dilman T., Giese U., Klüppel M., Kauts. Gummi Kunst., 2015, **68** (6) 69.
[13] Sengupta R., Bhattacharya M., Bandyopadhyay S., Bhowmick A. K., Prog. Polym. Sci., 2011, **36**, 638.
[14] Galimberti M., Coombs M., Cipolletti V., Riccio P., Ricco T., Pandini S., Conzatti L., Appl. Clay Science, 2012, **65**, 57.
[15] Galimberti M., Cipolletti V., Kumar V., Natural Rubber Based Composites and Nanocomposites. S. Thomas, C. H. Chan, L. A. Pothan, Ramanan, J. Maria Eds., Royal Soc. Chem., Chapter 2, 2014, 34.
[16] Ramorino G., Bignotti F., Conzatti L., Ricco T., Polym. Eng. Sci., 2007, **47** (10) 1650.
[17] Ramorino G., Bignotti F., Pandini S., Riccò T., Compos. Sci. Technol., 2009, **69**, 1206.
[18] Galimberti M., Coombs M., Riccio P., Ricco T., Passera S., Pandini S., Conzatti L., Ravasio A., Tritto I., Macromol. Mater. Eng., 2012, **298**, 241.
[19] Agnelli S., Cipolletti V., Musto S., Coombs M., Conzatti L., Pandini S., Riccò T., Galimberti M., eXPRESS Poly. Lett., 2014, **8** (6), 436.
[20] Galimberti M., Kumar V., Coombs M., Cipolletti V., Agnelli S., Pandini S., Conzatti L., Rubber Chem. Technol., 2014, **87** (2), 197.
[21] Kumar V., Giese U., Hanel T., Giannini L., Galimberti M., Kauts. Gummi Kunst., 2014, 67 (**10**), 38.
[22] Kumar V., Giese U., Hanel T., Giannini L., Galimberti M., Kauts. Gummi Kunst., 2014, 67 (**9**), 29.
[23] Donnet J. B., Custodero E., The Science and Technology of Rubber Third Ed. Mark JE Erman, Eirich FR, Eds. Elsevier Academic Press, Chapter 8, 2005, 367.
[24] Moewes M. M., Fleck F., Klueppel M., Rubber Chem. Technol., 2013, DOI: http://dx.doi.org/10.5254/rct.13.87930.
[25] Mauro M., Cipolletti V., Galimberti M., Longo P., Guerra G., J. Phys. Chem: C, 2012, **116**, 24809.
[26] Song S. H., Jeong H.K., Kang Y.G., J. Industrial Eng. Chem., 2010, 16 (**6**), 1059.
[27] Song S.H., Jeong H.K., Kang Y. G., Cho C.T., Korean J. Chem. Eng., 2010, **27**(4) 1296.
[28] Kusano T., JP, Bridgestone, 2004, 203342.
[29] Donnet J.B., Custodero E., in The Science and Technology of Rubber Third Ed.; Mark J.E., Erman B., Eirich F.R., Eds. Elsevier Academic Press 2005, Chapter 8, 367.
[30] Payne A.R., Whittaker R.E., Rubber Chem. Technol., 1971, **44**, 440.
[31] Robertson C.G., Roland CM, Rubber Chem. Technol., 2008, **81**, 506.
[32] Bohm G. A., Tomaszewski W., Cole W., Hogan T., Polymer, 2010, **51**, 2057.
[33] Heinrich G., Klüppel M., Adv. Polym. Sci., 2002, **160**, 1.
[34] Celzard A., Mareche J.F., Furdin G., Prog. Mater. Sci., 2005, **50** (1), 93.
[35] Medalia A.I., Rubber Chem.Technol., 1978, 51 (**3**) 437.
[36] Maier P.G., Goritz D., Kauts. Gummi Kunst., 1996, **49**, 18.
[37] Chazeau L., Brown J.D., Yanyo L.C., Sternstein S.S., Polym. Compos., 2000, **21**, 202.
[38] Sternstein S.S., Zhu A-J., Macromolecules, 2002, **35**, 7262.
[39] Montes H., Lequeux F., Berriot J., Macromolecules, 2003, **36**, 8107.
[40] Zhu Z., Thompson T., Wang S-Q., von Meerwall E.D., Halasa A., Macromolecules, 2005, **38**, 8816.
[41] Kalfus J., Jancar J., Polym. Compos., 2007, **28**, 365.
[42] Jancar J., Douglas J.F., Starr F.W., Kumar S.K, Cassagnau P., Lesser A.J., Sternsteinh S.S., Buehler M.J., Polymer, 2010, **51**, 3321.
[43] Funt J.M., Rubber Chem. Technol., 1988, **61**, 842.
[44] Gauthier C., Reynaud E., Vassoille R., Ladouce-Stelandre L., Polymer, 2004, **45**, 2761.
[45] Gold E., Phys. Rev., 1938, **53**, 322.
[46] Guth E., J. Appl. Phys., 1945, **16**, 20.
[47] Guth E., Rubber Chem. Technol., 1945, **18**, 595.